technical note technical note

Graphite Oxide Flame Retardants

March 2010

DOT/FAA/AR-TN09/60

U.S. Department of Transportation

Federal Aviation Administration

NOTICE

This report is available at the Federal Aviation Administration William J. Hughes Technical Center's Full-Text Technical Reports page: actlibrary.act.faa.gov in Adobe Acrobat portable document format (PDF).

Technical Report Documentation Page

1. Report No.	2. Government Accession No.	3. Recipient's Catalog No.
DOT/FAA/AR-TN09/60		

4. Title and Subtitle	5. Report Date
GRAPHITE OXIDE FLAME RETARDANTS	March 2010
	6. Performing Organization Code

7. Author(s)	8. Performing Organization Report No.
Amanda L. Higginbotham[1], Jay Lomeda[1], James M. Tour[1], Alexander B. Morgan[2], and Richard E. Lyon[3]	

9. Performing Organization Name and Address	10. Work Unit No. (TRAIS)
[1]Rice University 6100 Main Street, MS222 Houston, TX 77005 [2]University of Dayton Research Institute 300 College Park Dayton, OH 45469-0160	
	11. Contract or Grant No. 2007G010
[3]Federal Aviation Administration William J. Hughes Technical Center Airport and Aircraft Safety Research and Development Division Fire Safety Branch Atlantic City International Airport, NJ 08405	

12. Sponsoring Agency Name and Address	13. Type of Report and Period Covered
U.S. Department of Transportation Federal Aviation Administration Air Traffic Organization NextGen & Operations Planning Office of Research and Technology Development Washington, DC 20591	Technical Note
	14. Sponsoring Agency Code ANM-115

15. Supplementary Notes

16. Abstract

Thermoplastics and composites made from hydrocarbon polymers can improve the affordability, strength-to-weight ratio, and durability of manufactured products. Unfortunately, the use of these materials in aircraft and other vehicles is limited because of their inherent flammability. An alternative, lower-cost strategy is to develop environmentally benign additives that significantly reduce the flammability of commodity polymers. In this study, polymers blended with graphite oxide (GO) and its functionalized analogs were evaluated as cost-effective, fire-resistant materials for aircraft and other forms of mass transportation. GO polymer nanocomposites were prepared by dispersing 1, 2.5, 5, and 10 weight % GO in polycarbonate (PC), acrylonitrile butadiene styrene (ABS), and high-impact polystyrene (HIPS) for the purpose of evaluating the flammability and materials properties of the resulting systems. The overall morphology and dispersion of the GO within the polymer nanocomposites were studied by scanning electron microscopy and optical microscopy; the GO was found to be well-dispersed throughout the matrix without formation of large aggregates. Mechanical tests were performed using dynamic mechanical analysis to measure the storage modulus, which increased with GO loading for all polymer systems. Microscale oxygen consumption calorimetry revealed that GO could reduce the total heat release and heat release capacity of HIPS and ABS. Nanocomposites of GO with PC demonstrated very fast self-extinguishing times in vertical open flame tests. Heat release rate of the 2.5 weight percent GO nanocomposites measured in a cone calorimeter in flaming combustion was reduced 25% and a surface energy balance was used to explain the results in terms of enhanced radiant energy losses by the GO.

17. Key Words	18. Distribution Statement
Graphite oxide, Flame retardant, Nanocomposites	This document is available to the U.S. public through the National Technical Information Service (NTIS), Springfield, Virginia 22161.

19. Security Classif. (of this report)	20. Security Classif. (of this page)	21. No. of Pages	22. Price
Unclassified	Unclassified	26	

ACKNOWLEDGEMENTS

The authors are indebted to Natallia Safronava for microscale combustion calorimeter measurements, Wei Lu for preparation of the fire calorimeter samples, and Sean Crowley for fire calorimeter testing. Certain commercial equipment, instruments, materials, and companies are identified in this report to adequately specify the experimental procedure. This in no way implies endorsement or recommendation by the Federal Aviation Administration or William Marsh Rice University.

TABLE OF CONTENTS

LIST OF FIGURES

LIST OF TABLES

LIST OF SYMBOLS AND ACRONYMS

ε	Emissivity of polymer/nanocomposite surface
μ	Mass fraction of sample remaining at 850°C after thermal decomposition
q''_{ext}	External heat flux in fire or fire calorimeter
q''_{flame}	Flame heat flux into the surface
q''_{rerad}	Heat flux reradiated from the surface
ϕ	Area fraction of graphite oxide on burning surface
χ	Combustion efficiency of fuel gases in flame
h_c	Heat of complete combustion of volatile thermal decomposition products per unit starting mass of sample
H_c	Heat of complete combustion of volatile thermal decomposition products = $h_c/(1-\mu)$
H_c^{eff}	Effective heat of flaming combustion of volatile thermal decomposition products
T_p	Temperature at peak pyrolysis rate in a constant heating rate experiment
ABS	Acrylonitrile-butadiene-styrene terpolymer
$CHCl_3$	Chloroform
DMA	Dynamic mechanical analysis
GO	Graphite oxide
HIPS	High-impact polystyrene
HRC	Heat release capacity measured in MCC
HRR	Heat release rate
MCC	Microscale combustion calorimeter
PC	Polycarbonate
PTFE	Polytetraflouroethylene
SEA	Smoke extinction area
SEM	Scanning electron microscopy
TGA	Thermogravimetric analysis
THF	Tetrahydrofuran

EXECUTIVE SUMMARY

This report examines the efficacy of graphite oxide (GO) as a flame-retardant additive in commercial polymers (plastics). The nanometer-scale graphite oxide was blended with high-impact polystyrene, acrylonitrile-butadiene-styrene terpolymer, and polycarbonate; and the degree of dispersion of the GO in the resulting nanocomposites was quantified. Measurements were conducted to evaluate the mechanical, thermal, electrical, and flammability properties of these materials. Thermal combustion properties and flame resistance showed little or no improvement with the addition of GO, but the heat release rate in fire calorimetry tests was reduced by about 25% in polymers containing 2.5 weight percent GO. An engineering model was used to explain the reduction in heat release rate in the fire calorimetry experiments as a consequence of the re-emission of incident radiant energy by the GO that accumulates at the burning surface.

INTRODUCTION

PURPOSE.

In this study, polymers blended with graphite oxide (GO) and its functionalized analogs were evaluated as cost-effective, fire-resistant materials for aircraft and other forms of mass transportation.

BACKGROUND.

Thermoplastics and composites made from hydrocarbon polymers can improve the affordability, strength-to-weight ratio, and durability of manufactured products. Unfortunately, the use of these materials in aircraft and other vehicles is limited because of their inherent flammability. Over the years, the Federal Aviation Administration has been successful in responding to this challenge by fostering the development of engineering polymers that combine good mechanical and processing properties with low flammability. An alternative, lower-cost strategy is to develop environmentally benign additives that significantly reduce the flammability of commodity polymers. If successful, this approach would create new commercial opportunities for commodity plastics in public transportation.

EXPERIMENTAL

The polymers for this study were chosen because of their use in many engineering plastics applications; polycarbonate (PC) is somewhat inherently flame retardant due to its ability to form polyaromatics and release carbon dioxide upon ignition, while acrylonitrile-butadiene-styrene terpolymer (ABS) and high-impact polystyrene (HIPS) are considerably more flammable. Therefore, the wide-range of properties between the resins will allow for a broad evaluation of the ability of GO to reduce the flammability of commodity polymers. Nanocomposites were obtained by solvent-blending the treated GO with PC, ABS, and HIPS at various weight percent (%, w/w) loading levels.

MATERIALS.

POLYMER RESINS. HIPS (Dow Styron 478), ABS (Dow Magnum 9010), and PC (Dow Calibre 301-10) were obtained in pelletized form from original manufacturers as natural/unmodified resins and were used as received.

SYNTHESIS OF GRAPHITE OXIDE. GO was synthesized from expanded graphite obtained from SupraCarbonics, LLC using the Staudenmaier procedure [1 and 2]. Briefly, 5 g (416.7 mmol C) of expanded graphite was added in five portions to a stirred mixture of concentrated H_2SO_4 (87.5 mL) and fuming HNO_3 (45 mL) while cooling in an ice-water bath. $KClO_3$ (55 g, 0.45 mol) was added to this mixture in 11 separate and equal portions; each portion was added to the reaction mixture 15 minutes apart, while venting with nitrogen gas to reduce the risk of explosion upon generation of chlorine dioxide gas. Protective equipment, including face shields, acid-resistant gloves, and blast shields were used at all times. The resulting slurry was stirred at room temperature for 96 hours. The green slurry was poured into 4 L of ice water, and the mixture was filtered and subsequently washed with 5 L of 5% hydrogen choloride. The filter

cake was then rinsed thoroughly with water until the filtrate was neutral. The filter cake was then dispersed in methanol (300 mL, vigorous stirring) and precipitated with diethyl ether (350 mL) followed by a final, thorough rinse with diethyl ether to yield 4.1 g of a fine brown powder of GO.

FORMATION OF GO/HIPS NANOCOMPOSITES. The HIPS resin (10 g) was soaked overnight in 200 mL of tetrahydrofuran (THF) to expand and dissolve the polymer. Complete dissolution was achieved the next day by vigorous stirring with a metal spatula. In a separate container, GO (in the amount to reach the overall desired weight percentage in the system) was high-shear mixed for 30 minutes in ~100 mL THF. The GO/THF suspension was then poured into the dissolved HIPS/THF solution and high-shear mixed for 30 minutes. To precipitate the GO/HIPS polymer composite, the mixture was slowly added to a 5× volume of methanol (~1500 mL) with vigorous stirring. The GO/HIPS composite was isolated by filtering over a polytetraflouroethylene (PTFE) membrane (5-μm pore size), washed with methanol, and allowed to dry in air. Sample bars suitable for open-flame tests and dynamic mechanical analysis (DMA) were prepared via melt extrusion (CSI-183MMX Mini Max extruding system). The GO/HIPS composite was heated until molten and then extruded into a heated stainless steel mold (80°C, width 1.3 cm, length 7.6 cm, thickness 0.3 cm) at a processing temperature of 250°C.

FORMATION OF GO/ABS NANOCOMPOSITES. The ABS resin (10 g) was soaked overnight in 200 mL of chloroform ($CHCl_3$) to expand and dissolve the polymer. Complete dissolution was achieved the next day by vigorous stirring with a metal spatula. In a separate container, GO (in the amount to reach the overall desired weight percentage in the system) was high-shear mixed for 30 minutes in ~100 mL $CHCl_3$. The GO/$CHCl_3$ suspension was then poured into the dissolved ABS/$CHCl_3$ solution and high-shear mixed for 30 minutes. To precipitate the GO/ABS polymer composite, the mixture was slowly added to a 5× volume of diethyl ether (~1500 mL) with vigorous stirring. The GO/ABS composite was isolated by filtering over a PTFE membrane (5-μm pore size), washed with diethyl ether, and allowed to dry in air. Sample bars suitable for open-flame tests and DMA were prepared via melt extrusion (CSI-183MMX Mini Max extruding system). The GO/ABS composite was heated until molten and then extruded into a heated stainless steel mold (80°C, 1.3 cm width, 7.6 cm length, 0.3 cm thickness) at a processing temperature of 240°C.

FORMATION OF GO/PC NANOCOMPOSITES. The PC resin (10 g) was soaked overnight in 200 mL of THF to expand the polymer and begin dissolution. Complete dissolution was achieved the next day by vigorous stirring with a metal spatula and/or applying heat to the system. In a separate container, GO (in the amount to reach the overall desired weight percentage in the system) was high-shear mixed (IKA T-25 digital ULTRA-TURRAX® disperser with 18 G dispersing element, 7000 rpm) for 30 minutes in ~100 mL THF. The GO/THF suspension was then poured into the dissolved PC/THF solution and high-shear mixed for 30 minutes. To precipitate the GO/PC polymer composite, the mixture was slowly added to a 5× volume of methanol (~1500 mL) with vigorous stirring. The GO/PC composite was isolated by filtering over a PTFE membrane (5-μm pore size), washed with methanol, and allowed to dry completely. Sample bars suitable for open-flame tests and DMA were prepared via melt extrusion (CSI-183MMX Mini Max extruding system). The GO/PC composite was heated until

molten and then extruded into a heated stainless steel mold (80°C, 1.3 cm width, 7.6 cm length, 0.3 cm thickness) at a processing temperature of 270°C.

METHODS.

To determine the quality of the composites, the overall morphology and dispersion of GO were studied using scanning electron microscopy (SEM) and optical microscopy. In addition, mechanical properties of the composites were evaluated using DMA; the storage modulus and glass transition temperature were measured. To evaluate the thermal properties and flammability of the materials, microscale combustion calorimetry (MCC), thermogravimetric analysis (TGA), and open-flame resistance in a vertical orientation were performed.

SCANNING ELECTRON MICROSCOPY. SEM images were obtained at 5.0 kV on freeze-fractured cross sections of the respective GO/polymer composite sample bar. Before imaging, the samples were coated with a 20-nm layer of gold to minimize charging.

OPTICAL MICROSCOPY. The samples were imaged using a polarizing optical microscope (Zeiss Axioplan-2) by first melting a small portion of the polymer composite in an oven, and then pressing a thin layer onto a glass microscope slide.

DYNAMIC MECHANICAL ANALYSIS. DMA analysis (Q800, TA Instruments) was performed with a dual cantilever clamp on sample bars measuring 1.3 cm wide, 7.6 cm long, and 0.3 cm thick. A temperature ramp experiment (3°C/minute) was conducted under air from room temperature to 150°C (ABS and HIPS systems) or 180°C (PC systems) at a constant frequency of 1 Hz.

THERMOGRAVIMETRIC ANALYSIS. TGA analysis (Q50, TA Instruments) was conducted from room temperature to 950°C at 10°C/minute under argon purge gas flow of 200 cm^3/minute according to a standard method.

MICROSCALE COMBUSTION CALORIMETRY. MCC tests (MCC-1, Govmark) were run under nitrogen at a heating rate of 1°C/s from 250° to 750°C using method A of the standard test method ASTM D 7309 (pyrolysis under nitrogen) [3]. Each sample was tested in triplicate to evaluate reproducibility of the flammability measurements. The key thermal combustion properties measured during the 15-minute test are the heat release capacity (HRC) measured in MCC (J/g-K), which is the maximum specific heat release rate (W/g) measured in the test divided by the heating rate (K/s); the temperature at the maximum heat release rate T_p, the total heat of complete combustion of the fuel gases, h_c; and the mass fraction of the sample remaining after the test (pyrolysis residue), μ.

FLAME RESISTANCE IN VERTICAL ORIENTATION. The method used was a modified version of ASTM D 3801 [4]. Rectangular bars measuring 1.3 cm wide, 7.6 cm long, and 0.3 cm thick were tested in a draft-free cabinet (Atlas Electric HVUL-94 flame-test station). The methane tank pressure regulator was set to 23 psi; the pressure regulator on the HVUL-94 test station was set to 5 psi. The Bunsen burner flame height was 55 mm, and the height from the top of the Bunsen burner to the bottom of the test bar was 40 mm; therefore, the sample overlapped

with the flame by ~15 mm. All test bars underwent one trial, where the bar was exposed to a 10 s ignition, followed by flame removal, and the time to self-extinguishing was recorded.

FIRE TESTS. Fire response parameters were measured on 100- x 100- x 3-mm samples in a fire calorimeter operating on the oxygen consumption principle (Cone Calorimeter, Fire Testing Technology) according to standard method ASTM E 1354 [5] at an external heat flux of 50 kW/m^2 using an edge frame sample holder without a wire grid to prevent intumescence. Due to the difficulty of sample preparation, only a single test was conducted for each material.

RESULTS AND DISCUSSION

SAMPLE IMAGING.

SEM images (figure 1) taken of the composites at their fracture surface reveal that, overall, the GO flakes did not agglomerate into dense regions. GO flakes were present throughout, and no large, noticeable features were found, suggesting good dispersion. The images shown in figure 1 are for HIPS, ABS, and PC composites containing 10%, w/w GO. Flakes of GO, several microns in size, were found protruding from the polymer matrix and are indicated by the white arrows. Optical microscopy supports the SEM data but points to adequate dispersions at the microscale (figure 1, inset) due to the observation of dark regions, presumed to be GO, present in all parts of the sample. The concentration of the dark regions was not always evenly distributed, which may be attributed to the manner in which the optical samples were prepared; the polymer samples were heated to the point of softening and flattened on a glass microscope slide before imaging so that the light passing through the sample was maximized. Many regions were completely filled with GO and, thus, unable to be optically imaged.

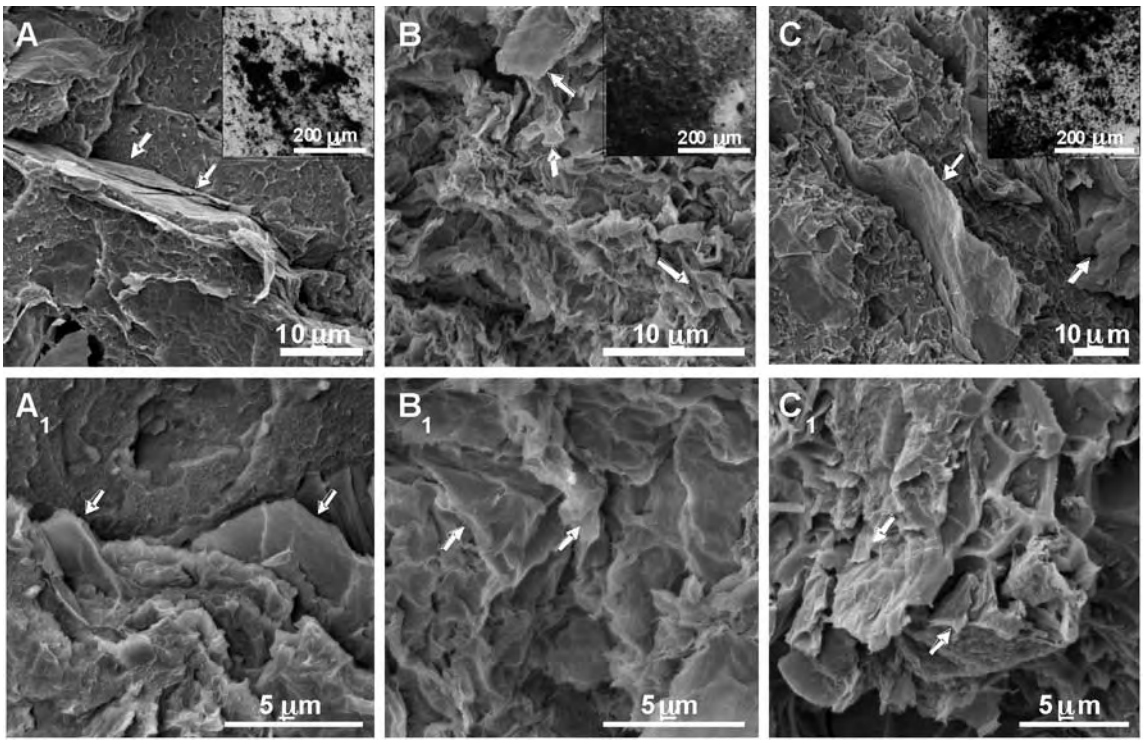

Figure 1. The SEM and Optical Microscopy Images (inset) of 10%, w/w GO loaded in (A) HIPS, (B) ABS, and (C) PC Composites (The bottom row of images shows zoomed-in regions of the sample directly above. White arrows highlight some of the areas that contain GO flakes. For all samples, it is apparent that the GO flakes did not form large agglomerates and are dispersed throughout all sample regions imaged.)

MECHANICAL PROPERTIES.

To study the effects of GO addition on the mechanical properties of the polymers, the storage modulus of the composites was measured using DMA. Not only is this of interest to determine the physical properties of the material, it may give insight to the flammability properties as well. One recent study indicated a direct relationship between viscoelastic measurement (storage modulus) and reduction in heat release rate (HRR) [6]. A dual cantilever clamp was used on sample bars measuring 1.3 cm wide, 7.6 cm long, and 0.3 cm thick; the samples were heated in air at 3°C/minute to 150°C (ABS and HIPS) or 180°C (PC). It was observed with all three polymers that the storage modulus increased with increasing GO content over the entire temperature range (figure 2). Though the increase in strength was not proportional to the amount of GO added, it is apparent that incorporation of the nanofiller did not deteriorate the mechanical properties of the polymer. The most distinct increase in storage moduli with increasing GO content was observed for HIPS, while PC showed only a small increase with 5%, w/w and 10%, w/w GO samples having almost identical storage modulus across the entire temperature range. The glass transition temperature (T_g) was extrapolated from the storage modulus data and did not vary significantly with increasing GO content. In general, the T_g increased slightly with increasing GO, which implies that GO addition increases the stiffness of the composites. The T_g for each sample is given in the inset of figure 2.

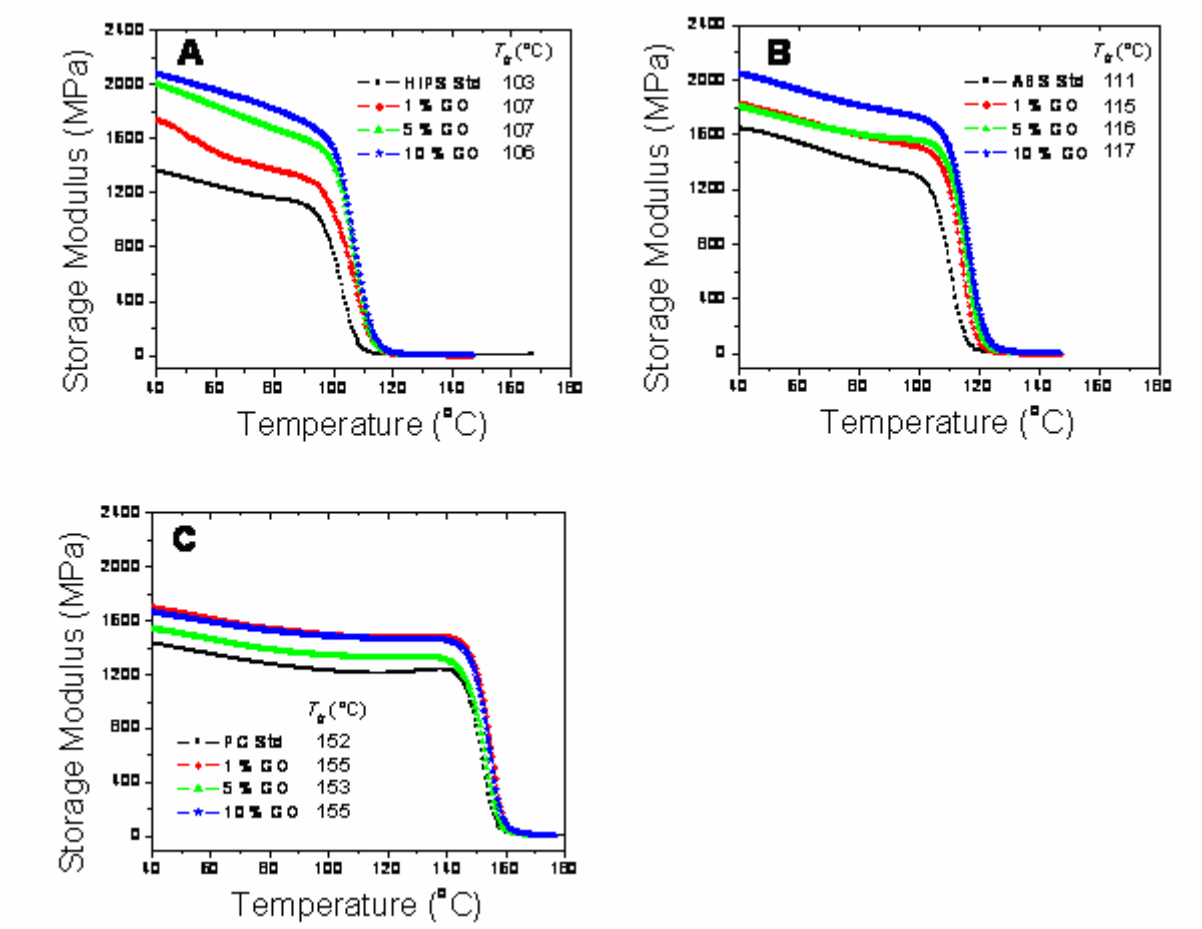

Figure 2. The DMA Storage Modulus With Increasing Temperature for GO Composites Made With (A) HIPS, (B) ABS, and (C) PC Systems (The T_g for each sample is shown in the inset. For all systems, the storage modulus increases with addition of GO over a wide temperature range.)

THERMAL STABILITY.

TGA was performed to assess the general thermal stability of the polymers and their GO composites. In general, the mass loss histories of the GO nanocomposites were not significantly different from the starting polymers. Table 1 gives the onset decomposition temperature, defined as the temperature at which 5%, w/w of the mass is lost, and the temperature of maximum weight loss rate (peak of the derivative curve) in the thermogravimetry experiments. For the HIPS systems, the temperatures remained fairly constant, except for the 5%, w/w GO sample, which increased both the decomposition onset and maximum weight loss rate temperatures (384° to 399°C and 423° to 426°C, respectively). For the ABS systems, both temperatures decreased slightly with increasing GO addition (381° to 371°C and 424° to 411°C for the 10%, w/w GO sample), indicating a slight decrease in thermal stability. Both temperatures for the PC systems remained constant for all GO loadings. Therefore, it can be concluded that GO addition does not significantly alter the thermal stability of the polymer resins to which it is added.

Table 1. Thermal Stability of HIPS, ABS, and PC With and Without GO at Various Loading Levels

Sample	Thermal Decomposition Temperature	
	Onset (°C)	Maximum Rate (°C)
HIPS Control	384	423
1% GO in HIPS	384	418
5% GO in HIPS	399	426
10% GO in HIPS	386	421
ABS Control	381	424
1% GO in ABS	374	413
5% GO in ABS	366	406
10% GO in ABS	371	411
PC Control	475	508
1% GO in PC	471	505
5% GO in PC	475	508
10% GO in PC	477	507

MICROSCALE COMBUSTION CALORIMETRY.

The MCC is a small-scale instrument that measures the heat release of a material by oxygen consumption calorimetry, which has been recently employed as a small-scale alternative to cone calorimetry when sample supply is limited [7]. The heat of combustion of pyrolysis products is measured, and the heat release can be used to predict the flammability of the material [8]. Using this technique, the samples are exposed to a fast heating rate to mimic fire-type conditions. The experiment consists of first pyrolyzing the sample under an inert atmosphere (nitrogen in this case) at a heating rate of 1°C/s from 250° to 750°C (using method A of ASTM D 7309), and then pushing the pyrolysis products into a 900°C combustion furnace where they are mixed with oxygen. The combustion gases from the furnace area then flow to an oxygen sensor, and the heat release is calculated based on the amount of oxygen consumed during the combustion process.

The results of the MCC tests are summarized in figure 3 and in table 2; there is a clear trend that as GO content increases, the total heat release and peak heat release capacity decreases. The one exception to this trend is for PC. PC is known to be sensitive to acids and bases such that the presence of acid or base can have negative effects on flame retardancy [9-11]. At low loading (1%, w/w), the effects of GO on heat release are minimal; but at 5%, w/w, a negative effect on flammability in both peak heat release and in total heat release was observed, likely caused by the acidic groups at a concentration high enough to result in PC molecular weight degradation and, therefore, a higher heat release (less PC polymer structure converts to char). At 10%, w/w GO, enough of a network structure had been formed that the GO could lower heat release/mass loss and counter the effects of the acidic groups on the GO surface. Perhaps with the exception

of PC, it appears the GO effectively decreased the flammability of the materials tested. However, while char yield increases as GO is increased, the collected char yields did not appear to be more than additive effects. In fact, it appears that about half the GO was consumed during the experiment, otherwise the char yields would be even higher, assuming 10%, w/w GO is thermally stable up to 900°C. An additional effect noted is that at 10%, w/w GO loadings, the polymer sample stops melting and flowing before becoming a char. The appearance of small black dots/char "lumps" (roughly in the shape of the starting sample) was noted in the 10%, w/w GO samples, which is a behavior also observed in carbon nanotube, carbon nanofiber, and clay nanocomposites with good nanoparticle dispersion and low heat-release behavior [12]. It is also a feature of a material with antidripping behavior (high-melt viscosity) during burning [6 and 13]. Additionally, the heat release rate curve shape is unchanged when comparing the control sample to the GO-containing samples. This indicates that the GO only slowed the rates of mass loss/fuel pyrolysis and most likely, did not change the thermal decomposition profile/chemistry of the sample.

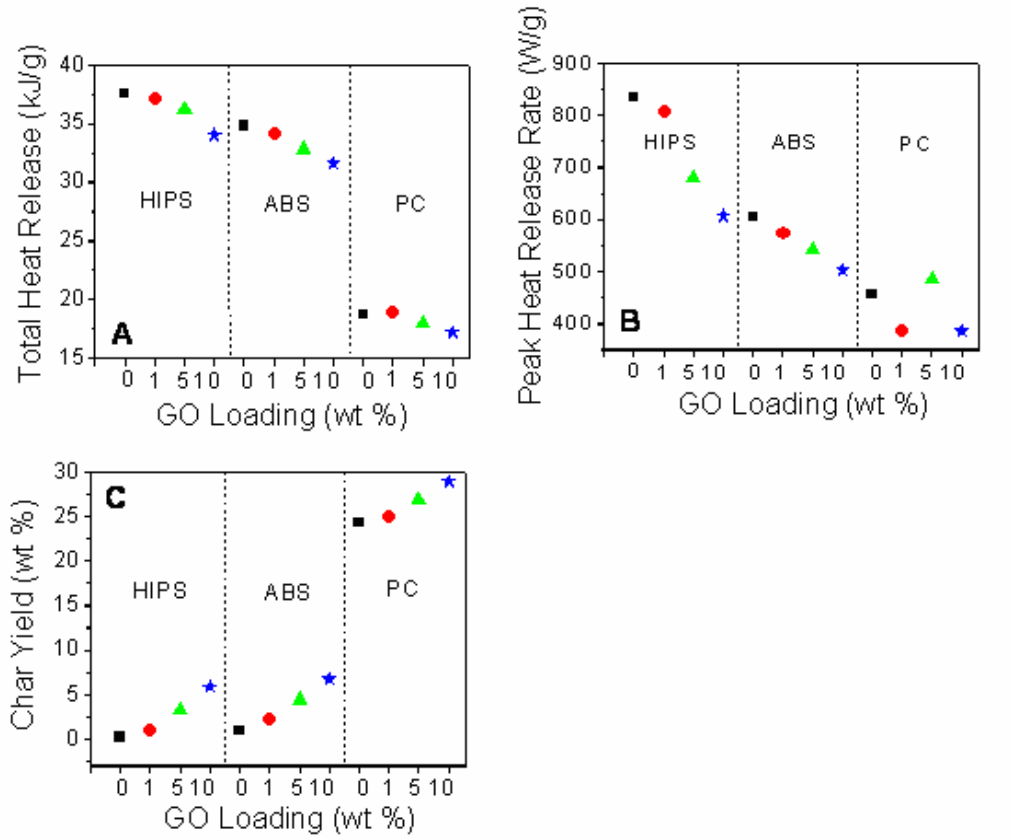

Figure 3. The MCC Results for GO-HIPS, GO-ABS, and GO-PC Nanocomposite Systems for (A) Total Heat Release, (B) Peak Heat Release Rate, and (C) Char Yield (There is a clear trend that the total heat release and peak heat release rate both decreased as GO content was increased in all polymers. The char yield also increased for all polymer systems as GO was increased, but this seems to be an additive effect.)

Table 2. Microscale Combustion Calorimetry Data for HIPS, ABS, PC, and Their Nanocomposites Containing 2.5% GO

Sample/Test	HRC, J/g-K	h_c, kJ/g	T_p, °C	μ
HIPS 1	892	37.6	447.8	0
HIPS 2	896	37.7	446.5	0
HIPS 3	874	37.7	448.2	0
HIPS Average	887	37.7	448	0.00
HIPA/GO 1	893	37.3	443.6	0.017
HIPS/GO 2	851	37.3	444.8	0.014
HIPS/GO 3	885	37.3	445.8	0.015
HIPS/GO Average	876	37.3	445	0.015
ABS 1	670	35.7	452	0.006
ABS 2	648	36	453.6	0.006
ABS 3	628	35.6	454.4	0.006
ABS Average	649	35.8	453	0.006
ABS/GO 1	571	33.5	436	0.039
ABS/GO 2	594	33.5	436	0.036
ABS/GO 3	576	33.5	436.7	0.037
ABS/GO Average	580	33.5	436	0.037
PC 1	465	20	528.3	0.214
PC 2	432	20.6	515	0.211
PC 3	503	20.3	523.7	0.209
PC Average	467	20.3	522	0.211
PC/GO 1	577	20.8	518.5	0.222
PC/GO 2	537	20.5	525.4	0.217
PC/GO 3	528	21.4	527.7	0.220
PC/GO Average	547	20.9	524	0.220

FLAME RESISTANCE.

The resistance of a thin sample to upward flame propagation after brief exposure to a Bunsen burner (flame resistance) was performed on polymer nanocomposites molded into the shape of a rectangular bar (1.3 cm wide, 7.6 cm long, and 0.3 cm thick). In the test, the bar was suspended above a cotton patch in a draft-free enclosure and was exposed for 10 s to a premixed, methane-air flame. After the 10-s ignition period, the flame was removed and the time for the polymer to self-extinguish was recorded. Sample dripping and cotton ignition were also noted. The test performed was a modified version of ASTM D 3801. Based on the actual flame height that was used, the test method can be classified as being between the UL-V0 (ASTM D 3801) and UL-94 5V (ASTM D 5048) tests in severity [4]. These methods typically give ratings of V-0,

V-1, V-2 to materials based on self-extinguishing time and dripping behavior; however, since the method used was not an exact match to the UL-94 specifications, such assignments could not be made. Unlike MCC, this type of test can provide a general assessment as to how GO affects the material's drip behavior in a flaming drip fire risk scenario, which is important to industrial fire safety applications. The vertical fire test results for all composites are summarized in table 3. As expected, the GO-PC composites displayed the best results; the self-extinguishing times for 5% and 10%, w/w GO in PC were immediate after removal of the flame. Although the self-extinguishing times of ABS systems were considerably longer, the behavior of the burning material suggests flame-retarding behavior with increasing GO content. The ABS standard (no GO present) began elongating almost immediately after removal of the flame until almost the entire sample dripped after 68 s. With only 1%, w/w GO in ABS, the sample did not elongate as drastically. After ~20 s, a small portion of the sample dripped (and ignited the cotton), but most of the sample remained and extinguished immediately after the drip occurred. Similar behavior was observed for 5% and 10%, w/w GO in ABS; elongation was diminished such that dripping was only limited to a small portion of the sample and the remaining sample self-extinguished. As expected, the HIPS samples, being the most flammable starting material, performed worst in the flame tests. The standard dripped several times (the first time only 12 s after the flame was removed) and never self-extinguished. The addition of GO to HIPS only increased the amount of time until the first drip; all samples continued burning, even after portions had dripped, until the entire sample was completely consumed.

Table 3. Flame Resistance in Vertical Burning Test

Sample	Time to Self-Extinguish (s)	Observed Dripping	Time Before First Drip (s)	Sample Remaining	UL-94 V Rating*
HIPS Control	n/a	Yes	12	No	NR
1% GO in HIPS	n/a	Yes	14	No	NR
5% GO in HIPS	n/a	Yes	17	No	NR
10% GO in HIPS	n/a	Yes	24	No	NR
ABS Control	68	Yes	68	Yes	NR
1% GO in ABS	21	Yes	68	Yes	NR
5% GO in ABS	33	Yes	33	Yes	NR
10% GO in ABS	79	Yes	79	Yes	NR
PC Control	14	Yes	14	Yes	V2
1% GO in PC	4	No	n/a	Yes	V0
5% GO in PC	0	No	n/a	Yes	V0
10% GO in PC	0	No	n/a	Yes	V0

*Projected value based on test results.
NR = No vertical rating

Despite the poor flame test results for ABS and HIPS, it appears that GO is still an effective additive for lowering the HRR of host polymers. In fact, it has been shown that nanocomposites may lower HRR while giving poor flammability test results in similar UL-94 [14]. Further, the HRR and vertical fire test results do not correlate [15]. This is important to note since open-flame tests do not measure HRR nor do they suggest that the material will provide a high level of fire safety in all fire risk scenarios. However, the observations of the sample behavior on burning with this open-flame test combined with MCC and TGA data demonstrate the ability of GO to act as a flame-retardant additive.

FIRE BEHAVIOR.

Fire calorimetry test results of the pure HIPS, ABS, and PC controls and the 2.5% GO nanocomposites are given in table 4, including time to ignition, peak HRR, time to peak HRR, test average HRR, effective heat of flaming combustion of the fuel gases (H_c^{eff}), and smoke production expressed as the test average specific smoke extinction area (SEA). The combustion efficiency of the fuel gases in the flame χ is the ratio of the effective heat of combustion in the fire calorimeter to the total heat of complete combustion of the fuel gases in the MCC, i.e., $\chi = (1-\mu) H_c^{eff} / h_c$. These combustion efficiencies, which are listed in the last column of table 4, correlate with the SEA values in that more visible smoke (which is a product of incomplete combustion) is observed for the HIPS and ABS materials that have lower χ values. The HRR histories of the polymers and nanocomposites from which the data in table 3 were obtained are shown in figure 4. Visual observation of the test specimens after the fire calorimetry tests showed that the GO formed a discontinuous, friable, low-density residue that covered about 1/3 of the original 100-cm^2 surface area of the specimen.

Table 4. Fire Calorimetry Results for HIPS, ABS, PC, and Their Nanocomposites With 2.5% GO

Sample	Time to Ignition (s)	Peak HRR (kW/m^2)	Time to Peak HRR (s)	Average HRR (kW/m^2)	H_c^{eff} (MJ/kg)	Average SEA (m^2/kg)	χ
HIPS	32	1108	101	336	30.2	1246	080
HIPS/GO	16	858	114	346	29.8	1289	0.79
ABS	24	980	109	296	28.5	1178	0.79
ABS/GO	20	649	69	258	28.0	1214	0.80
PC	34	600	119	257	21.7	626	0.84
PC/GO	28	470	89	213	23.5	530	0.88

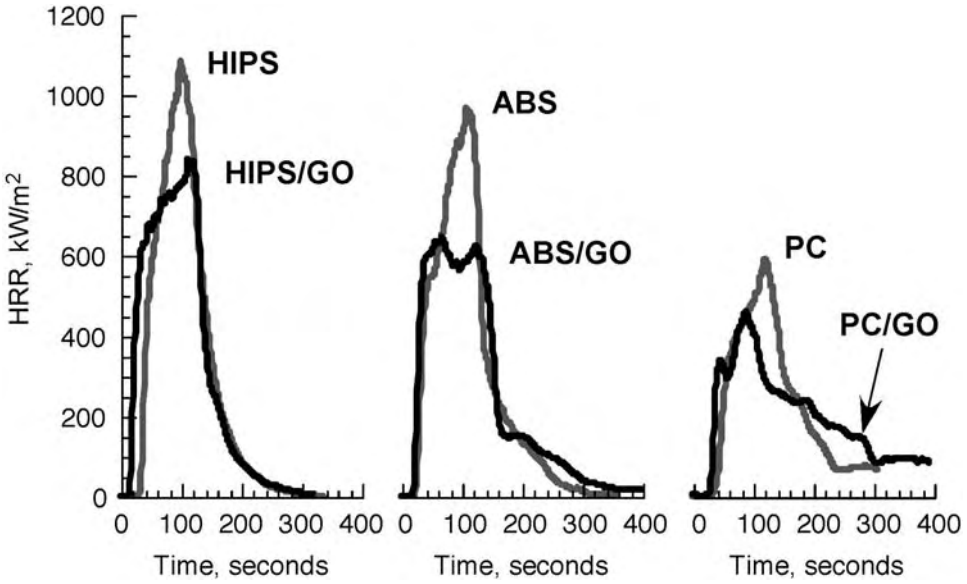

Figure 4. Heat Release Rate Histories for HIPS, ABS, PC (grey curves), and Their Nanocomposites Containing 2.5% GO (black curves)

FLAME-RETARDANT MECHANISM OF GO.

The reduction in HRR of polymer-GO nanocomposite samples, as observed in table 4 and figure 4, is thought to be due to the ability of GO to form a protective surface residue that acts as a thermal insulator and a mass transport barrier [16]. To distinguish between heat and mass transport as a mechanism for reduced HRR by GO, a one-dimensional burning model with an ablative surface boundary condition (no mass diffusion) was used to interpret the HRR results [17]:

$$HRR = \chi \frac{H_c}{H_g} q''_{net} = \frac{H_c^{eff}}{H_g}\left(\varepsilon q''_{ext} + \varepsilon q''_{flame} - q''_{rerad}\right) \quad (1)$$

In equation 1, H_c is the heat of complete combustion of the fuel gases; $H_c^{eff} = \chi H_c$ is the effective heat of flaming combustion; H_g is the energy required to liberate unit mass of volatile fuel at the burning surface (heat of gasification); q''_{net} is the net surface heat flux in units of W/m^2 expressed in terms of the incident heat flux from an external radiant heater or fire, q''_{ext}, the heat flux to the surface from the attached flame, q''_{flame}, and the reradiated heat flux, q''_{rerad}.

When GO nanocomposites burn in one-dimensional, horizontal flaming combustion, GO accumulates at the surface. If the GO is present in concentrations at or above the percolation threshold [18], the accumulated GO will form a continuous, porous graphitic layer, otherwise the GO will accumulate into discreet regions. In either case, the GO is thermally stable and can sustain a much higher temperature than the polymer matrix, which thermally decomposes and burns around it. Consequently, the GO nanoparticles absorb and reradiate more of the incident energy to the environment than the polymer matrix and q''_{net}, which drives the burning process, is reduced accordingly. To evaluate the magnitude of surface reradiation associated with GO,

assume that the GO in the burning nanocomposite surface aggregates into regions that are in thermal equilibrium with the radiant heater in the fire calorimetry tests, so that the reradiated heat flux per unit area of GO q''^{go}_{rerad}, having emissivity ε_{GO}, is related to the external heat flux, $q''^{go}_{rerad} = \varepsilon_{GO}\, q''_{ext}$. If the total surface reradiation is the area-weighted-fraction of the reradiated fluxes of the GO and the surrounding polymer and ϕ is the area fraction of GO,

$$q''_{rerad} = \phi\, q''^{go}_{rerad} + (1-\phi) q''^{poly}_{rerad} \tag{2}$$

Since the polymer burns (reradiates) at a temperature that is close to its onset thermal decomposition temperature T_{onset} [19], $q''^{poly}_{rerad} \approx \varepsilon_p \sigma\ T^4_{onset}$ with ε_p representing the polymer surface emissivity and σ = 5.7 x 10^{-8} W/m^2-K^4 the Stefan-Boltzmann radiation constant. If the emissivity of the carbon nanotube residue is typical of burning polymers, then $\varepsilon_{GO} = \varepsilon_p = \varepsilon \approx 1$ [20 and 21] and equation 1 becomes

$$HRR\ =\ (1-\phi)\frac{H^{eff}_c}{H_g}\left(q''_{ext} - \sigma T^4_{onset}\right) +\ \frac{H^{eff}_c}{H_g} q''_{flame} \tag{3}$$

Equation 3 was evaluated for each polymer and GO nanocomposite at the external heat flux used in the experiments, q''_{ext} = 50 kW/m^2 with the onset thermal degradation temperatures T_{onset} in table 1, the average effective heat of combustion H^{eff}_c in table 4, and a typical heat of polymer gasification, H_g = 1600 J/g [22]. With these parameters specified, the flame heat fluxes were adjusted so that the calculated peak HRR of the pure polymers (ϕ = 0) agreed with the measured values. The empirical flame heat fluxes obtained were q''_{flame} = 10 kW/m^2 for PC and PC/GO; q''_{flame} = 14 kW/m^2 for ABS and ABS/GO; and q''_{flame} = 20 kW/m^2 for HIPS and HIPS/GO, all of which are typical of flame heat fluxes for polymers in cone calorimeters [19]. With the thermal combustion parameters and flame heat fluxes specified, equation 3 was used to calculate the peak HRR of the HIPS, ABS, and PC nanocomposites as a function of effective surface area fraction ϕ of the GO nanoparticles for the samples of this study.

The calculated peak HRRs are shown in figure 5 as solid and dashed lines. The measured peak HRRs are shown as circles located at the flame heat flux calibration value (ϕ = 0) and at the value of ϕ for each nanocomposite that coincides with its semi-empirical line. It is clear that the value of ϕ that correlates the experimental data for the 2.5%, w/w nanocomposites with the theoretical lines are ϕ = 0.37, 0.47, and 0.30 for HIPS, ABS, and PC, respectively. These values are in the range of the area fraction of the GO residue observed at the end of the fire calorimetry test, i.e., about 1/3 of the original surface area.

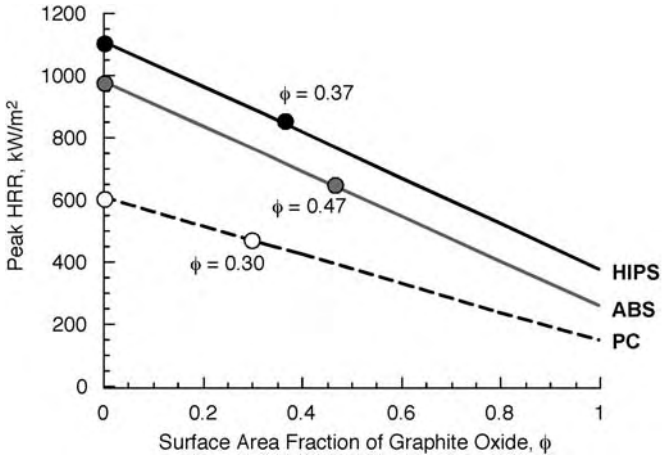

Figure 5. Peak HRR of HIPS, ABS, PC, and Their Nanocomposites Versus Surface Area Fraction of GO (The lines are calculated values. Circles are measured values.)

Figure 5 shows that complete coverage of the burning surface by a continuous network ($\phi = 1$) of GO particles would be expected to reduce the peak HRR by about a factor of 3-4, as is commonly observed for well-dispersed nanoparticle-polymer composites [23-27]. Based on visual observation of the samples after the MCC tests (see MCC Results section), a continuous network ($\phi = 1$) was expected at loading levels of 10%, w/w GO in the HIPS, ABS, and PC polymers of the present study, similar to what was observed for well-dispersed, nanometer-sized clay particles [23 and 24] which also have a plate-like geometry.

CONCLUSIONS

Graphite oxide (GO) was blended at 1, 2.5, 5, and 10 weight percent (%, w/w) in the commodity polymers high-impact polystyrene (HIPS), acrylonitrile-butadiene-styrene terpolymer (ABS), and polycarbonate (PC) to serve as a flame-retarding nano-additive. Scanning electron and optical microscopy showed that the GO was well dispersed throughout the composite. Dynamic mechanical analysis revealed that GO increases the storage modulus and the glass transition temperature, of the polymer. GO had little effect on thermal combustion properties of milligram samples or the flame resistance of 3-mm-thick samples, probably because thermal protection by re-emission of incident radiant energy was precluded by the nature of these tests. The peak heat release rate (HRR) in fire calorimeter tests of 3-mm-thick samples of HIPS, ABS, and PC containing 2.5%, w/w GO was reduced by about 25%, which was significantly greater than can be accounted for by the mass fraction. An energy balance was used to explain the observed effect in terms of surface re-emission of incident radiant energy by the GO, which covers about 1/3 of the surface at the 2.5% loading level of the samples tested in the fire calorimeter. Although the 25% reduction in peak HRR of the GO nanocomposites is significantly greater than the mass fraction of GO can account for on an additive basis, it is only about a third of what would be expected for a continuous nanoparticle (percolated) network. This could be due to a number of factors, such as (1) insufficient GO mass/volume fraction at the surface of thin samples to form a continuous reradiating layer, (2) the absence of a percolated nanoparticle network in the as-prepared nanocomposites, or (3) a percolated network with low strength due to the shape or aspect ratio of the dispersed GO.

REFERENCES

1. McAllister, M.J., Li, J.L., Adamson, D.H., Schniepp, H.C., Abdala, A.A., Liu, J., Herrera-Alonso, M., Milius, D.L., Car, R., Prud'homme, R.K., and Aksay, I.A., *Chemistry of Materials*, Vol. 19, 2007, pp. 4396-4404.

2. Staudenmaier, L., *Ber. Dtsch. Chem. Ges.*, Vol. 31, 1898, pp. 1481-1487.

3. American Society of Testing and Materials, "Standard Test Method for Determining Flammability Characteristics of Plastics and Other Solid Materials Using Microscale Combustion Calorimetry," ASTM D 7039, West Conshohocken, Pennsylvania, 2007.

4. American Society of Testing and Materials, "Standard Test Method for Measuring the Comparative Burning Characteristics of Solid Plastics in a Vertical Orientation," ASTM D 3801, West Conshohocken, Pennsylvania, 2006.

5. American Society of Testing and Materials, "Standard Test Method for Heat and Visible Smoke Release Rates for Materials and Products Using an Oxygen Consumption Calorimeter," ASTM E 1354, West Conshohocken, Pennsylvania, 2004.

6. Kashiwagi, T., Du, F., Douglas, J.F., Winey, K.I., Harris, R.H., and Shields, J.R., "Nanoparticle Networks Reduce the Flammability of Polymer Nanocomposites," *Nature Materials*, Vol. 4, 2005, pp. 928-933.

7. Morgan, A.B. and Galaska, M., "Microcombustion Calorimetry as a Tool for Screening Flame Retardancy in Epoxy," *Polymers for Advanced Technologies*, Vol. 19, Issue 6, 2008, pp. 530-546.

8. Lyon, R.E. and Walters, R.N., "Pyrolysis Combustion Flow Calorimetry," *Journal of Analytical and Applied Pyrolysis*, Vol. 71, 2004, pp. 27-46.

9. Grause, G., Sugawara, K., Mizoguchi, T., and Yoshioka, T., "Pyrolytic Hydrolysis of Polycarbonate in the Presence of Earth-Alkali Oxides and Hydroxides," *Polymer Degradation and Stability*, Vol. 94, Issue 7, 2009, pp. 1119-1124.

10. Levchik, S.V. and Weil, E.D., "Overview of Recent Developments in the Flame Retardancy of Polycarbonates," *Polymer International*, Vol. 54, Issue 7, 2005, pp. 981-998.

11. Levchik, S.V. and Weil, E.D., "Flame Retardants in Commerical Use or in Advanced Development in Polycarbonates and Polycarbonate Blends," *Journal of Fire Sciences*, Vol. 24, 2006, pp. 137-151.

12. Morgan, A.B., "Flame Retarded Polymer Layered Silicate Nanocomposites: A Review of Commercial and Open Literature Systems," *Polymers for Advanced Technologies*, Vol. 17, Issue 4, 2006, pp. 206-217.

13. Kashiwagi, T., Du, F., Winey, K.I., Groth, K.M., Shields, J.R., Bellayer, S.P., Kim, H., and Douglas, J.F., "Flammability Properties of Polymer Nanocomposites With Single-Walled Carbon Nanotubes: Effects of Nanotube Dispersion and Concentration," *Polymer*, Vol. 46, No. 2, 2005, pp. 471-481.

14. Bourbigot, S., Duquesne, S., Fontaine, G., Bellayer, S., Turf, T., and Samyn, F., "Characterization and Reaction to Fire of Polymer Nanocomposites With and Without Conventional Flame Retardants," *Molecular Crystals and Liquid Crystals*, Vol. 486, 2008, pp. 325-339.

15. Morgan, A.B. and Bundy, M., "Cone Calorimeter Analysis of UL-94 V-Rated Plastics," *Fire and Materials*, Vol. 31, Issue 4, 2007, pp. 257-283.

16. Kashiwagi, T., "Progress in Flammability Studies of Nanocomposites With New Types of Nanoparticles," *Flame Retardant Polymer Nanocomposites*, Morgan, A.B. and Wilkie, C.A., eds., John Wiley & Sons, Inc., Hoboken, New Jersey, 2007, pp. 285-324.

17. Tewarson, A., "Generation of Heat and Chemical Compounds in Fires," *SFPE Handbook of Fire Protection Engineering*, 3rd ed., National Fire Protection Association, Quincy, Massachusetts, 2002, Section 3, pp. 82-162.

18. Xia, W. and Thorpe, M.F., "Percolation Properties of Random Ellipses," *Physical Review A*, Vol. 38, No. 5, 1988, pp. 2650-2656.

19. Lyon, R.E., "Plastics and Rubber," *Handbook of Building Materials for Fire Protection*, C.A. Harper, ed., McGraw-Hill, New York, Chapter 3, 2004, pp. 3.1-3.51.

20. Stoliarov, S.I., Crowley, S., Lyon, R.E., and Linteris, G.T., "Prediction of the Burning Rates of Non-Charring Polymers," *Combustion and Flame*, Vol. 156, 2009, pp. 1068-1083.

21. Hallman, J.R., Welker J.R., and Sliepcevich, C.M., "Polymer Surface Reflectance-Absorbance Characteristics," *Polymer Engineering and Science*, Vol. 14, 1974, pp. 717-723.

22. Stoliarov, S.I. and Walters, R.N., "Determination of the Heats of Gasification of Polymers Using Differential Scanning Calorimetry," *Polymer Degradation & Stability*, Vol. 93, 2008, pp. 422-427.

23. Morgan, A.B. and Wilkie, C.A., eds., *Flame Retardant Polymer Nanocomposites*, John Wiley & Sons, Hoboken, New Jersey, 2007.

24. Kashiwagi, T., Danyus, R., Liu, M., Zammarano, M., and Shields, J.R., "Enhancement of Char Formation of Polymer Nanocomposites Using a Catalyst," *Polymer Degradation and Stability*, Vol. 94, 2009, pp. 2028-2035.

25. Schartel, B., "Considerations Regarding the Specific Impacts of the Principal Fire Retardancy Mechanisms in Nanocomposites," *Flame Retardant Polymer Nanocomposites*, Morgan, A.B. and Wilkie, C.A., eds., John Wiley & Sons, Hoboken, New Jersey, 2007, pp. 107-129.

26. Kashiwagi, T., Shields, J.R., Harris, R.H., and Awad, Jr., W.H., "Flame Retardant Mechanism of a Polymer Clay Nanocomposite," *Recent Advances in Flame Retardancy of Polymers*, Lewin, M., ed., Vol. 14, Business Communications Co., Norwalk, Connecticut, 2003, pp. 14-26.

27. Liu, X., "Flammability Properties of Clay-Nylon Nanocomposites," Masters Thesis, University of Maryland, Department of Fire Protection Engineering, College Park, Maryland, August 18, 2004.